ISSN 2176-5480

22nd International Congress of Mechanical Engineering (COBEM 2013)
November 3-7, 2013, Ribeirão Preto, SP, Brazil

THE EFFECTS OF MICROSTRUCTURE AND HARDNESS OF HYPOEUTECTIC AL-SI ALLOYS OVER THEIR MACHINABILITY

Eduardo Tadeu Schiavon Gandini
eduardo.gandini@aiesec.net
Bruno Monte Carmelo Donadoni
brunomcdonadoni@hotmail.com
Armando Ítalo Sette Antonialli
antonialli@ufscar.br
José Eduardo Spinelli
spinelli@ufscar.br

Department of Materials Engineering
Federal University of São Carlos
Washington Luís at km 235
São Carlos - SP - Brazil
CEP 13565-905

Abstract. *Almost 90% cast aluminum products are based on the aluminum-silicon system due to their excellent castability and interesting mechanical properties. A number of papers in the literature relate some microstructural features to their hardness, yield or ultimate tensile strength, but there is a lack of studies highlighting the effects of those variables over their machinability. In this study, Al-5.0wt.%Si and Al-9.0wt.%Si ingots were produced by horizontal directional solidification apparatus in order to achieve a broad microstructural spectrum, i.e., a considerable range of tertiary dendrite arm spacing, λ_3. The Al-Si alloy castings were then sectioned into five segments, which were submitted to end milling cutting force tests using a multicomponent dynamometer. In both evaluated Al-Si alloys, experimental correlations were adopted for representing the total milling cutting force dependency on λ_3 and Vickers hardness. Results show that finer as-cast microstructure requires maximum cutting force, and higher values for interdendritic spacing clearly reduce this demand. A stable level of cutting forces is found where tertiary arm spacing reaches above 50 µm for the Al-5.0wt%Si alloy.*

Keywords: *aluminum cast alloys, horizontal directional solidification, tertiary dendrite arm spacing, machinability.*

1. INTRODUCTION

Aluminum–silicon alloys are widely used in internal combustion engine components (Santos, 2007). Commercial alloys such as Al 356.0 (Al-7Si-0.3Mg) and Al 390.0 (Al-17.0Si-4.5Cu-0.6Mg) were developed for engine in order to reduce vehicle weight (Ye, 2003). Relative low melting point of such alloys tends to assist their processability by gravity and die casting techniques. The manufacturing of piston for internal combustion engines, for instance, is made using hypoeutectic, eutectic and hypereutectic aluminum–silicon alloys.

The range of silicon may roughly vary from 7 to 18 wt.%. Al-Si based engine blocks for instance have a very complex geometry to be achieved. Such parts have to be initially cast and thereafter subject to machining. It can be inferred that the final as-cast microstructure affects decisively machining behavior of such alloys. Indeed, high wear-resistant tools have to be developed (polycrystalline diamond, PCD and carbide) due to strong abrasive action on tool induced by Si particles, which difficult machining operations (Wang, 2012). Once again, one can infer that shape, distribution and size of Si particles may decisively affect machining performance of Al-Si alloys.

When a hypoeutectic Al-Si alloy solidifies, the primary aluminum forms and grows in dendrites or silicon phase forms and grows in angular primary particles. When the eutectic point is reached, the eutectic Al-Si phases nucleate and grow until the end of solidification. At room temperature, hypoeutectic alloys consist of a soft and ductile primary aluminum phase and a hard and brittle eutectic silicon phase (Ye, 2003). A dendritic arrangement of the primary Al-rich phase is quite common to be observed. Dendrite arm spacing as well as the size of Si particles, i.e., microstructure scale, strongly depends on solidification behavior. Such behavior can be translated by kinetic parameters such as tip growth rate (V_L) and cooling rate (T).

Silicon (Si) particles are normally formed as needles enveloping dendritic matrix. However, modifiers like Na, Sr and Sb can be added in order to modify the shape from needle-like to fiber-like. Although improve in mechanical properties due to such modification is well known (Rathod and Manghani, 2012), the effects of both size of silicon particles and their morphologies on machinability of Al-Si parts remain unknown. Thus, this understanding means a task to be accomplished by research teams in Academy or Industry.

Mechanical strength and ductility are influenced by the dimensions and continuity of the primary/secondary/tertiary dendritic branches (Donelan, 2000; Chemingui, 2010; Osório, 2006; Santos, 2007; Osório, 2007; Goulart, 2006 and

ISSN 2176-5480

2007). Goulart and co-authors stated that ultimate tensile strength on Al-5.0 and 9.0wt%Si alloys increases with decreasing secondary dendrite arm spacing, while yield strength seems to be independent of both the dendritic arrangement and of alloy composition. Under stress, the Al-rich phase deforms whereas cracks develop in the silicon, the tendency of crack formation increasing with increasing silicon particle size. Other than, Campbell (2003) stated that dendrite arm spacing usually refers to the spacing between the secondary arms of dendrites. However, if tertiary arms (λ_3) were present at a smaller spacing, then it would refer to this. The availability of studies on tertiary dendrite arms is very restricted. Tertiary dendrite arms may probably contribute with a more homogeneous distribution of the Al-rich phase.

Recent study developed by Sokołowski and co-authors (2006) has shown that in the case of high speed milling (HSM) operations of Al-Si sand casting (under constant speed, feed, and axial depth-of-cut) surface roughness is a function of both the silicon content and morphology of silicon phase. It was demonstrated that an increase in the resultant cutting force degrades the machined surface finish.

Santos and co-authors (2007) in their research work evaluated behavior of a diamond like carbon (DLC) coated cemented carbide cutting tool against Al-Si alloys. Turning tests were run for Al-Si alloys with 12 wt. % and 16 wt. % of silicon. The feeding force is higher for the Al-16wt%Si alloy. According to the authors, this is due to the presence of a fraction of 5% of non-eutectic silicon plates which increases the amount of aluminum adhesion in the cutting edge of the tool. On the other hand, the cutting force is neither affected by DLC deposition on the nor by the silicon content in the aluminum alloys.

The molten Al-12wt. %Si alloy was degasified and modified with sodium while the Al-16wt.%Si alloy was degasified and refined with phosphorous. Both Al-Si alloys were casted in a gray cast iron permanent mold. The hardness of both Al-Si alloys was around 30 HRB. Additionally, it was stated by Santos and co-authors (2007) that the cutting force shows minor difference if compared both examined chemistries. The average cutting force value was about 55N.

Zedan and co-authors (2010) selected T6 heat-treated 396 alloys (containing ~11wt. % Si), and B319.2 and A356.2 alloys (containing ~7wt. % Si) in order to perform drilling. It was found that alloys containing higher silicon content required greater cutting force for the same level of Mg and very close Brinell hardness values of about 108HB. In terms of the number of holes drilled, such results indicate that the silicon content has little effect on the tool life.

Zedan et al. (2010) stated that there is a need for bridging the boundary between casting process and machining operations, with a view of examining various aspects affecting the machinability of Al-Si casting alloys. The term machinability may be taken to imply that there is a property or quality of any given material which can be clearly defined and quantified, thus indicating how easy (or difficult) that mechanical operation can be. In fact, that term is not unambiguous, but the machinability of a material can be assessed by employing criteria such as: (i) tool life or limiting rate of metal removal; (ii) surface finish and chip morphology and (iii) cutting forces or power consumption (Trent and Wright, 2000). Machinability can be compared by different ways and is determined by several different types of tests. For example, the cutting force test measures the main cutting force necessary to machine any material under standardized conditions. The lower the force, the more machinable is the material (Zimmerman, Boppana and Katbi, 1990).

The purpose of this study is to perform transient horizontal solidification experiments of two hypoeutectic Al-5.0 and 9.0wt. %Si alloys view to permitting the effects of Si content and cooling rate on the final tertiary dendritic arrangement. Other goal includes assessing the effects of tertiary dendritic spacing on milling cutting force and hardness especially in the case of the Al-5.0wt. %Si alloy.

2. EXPERIMENTAL PROCEDURE

In order to assess some correlation between dendrite arm spacing of hypoeutectic cast aluminum-silicon alloy and its machinability, it was necessary to achieve a broad microstructural spectrum for both the Al-5.0 and 9.0wt.%Si alloys, which was feasible due to the construction of a horizontal directional solidification apparatus The produced ingots were then prepared to cutting force tests. See items below.

2.1 Horizontal directional solidification

The horizontal solidification device was initially designed. A copper mold was machined to the following specifications: 90 mm of height, 85 mm of width and 60 mm of length. The refractory fibrous plates had 1 (one) inch in width and were cut as to fit the copper mold in one of the sides of the box. The plates were sanded to better match the ideal size and were glued together and coated with an alumina based suspension.

Holes were made for the thermocouples, initially 3mm from the mold, then more 5 holes 10mm apart each and the last one 20mm in distance (a steel plate was made with the same hole measurements to better fix the thermocouples) as can be seen in Fig. 1. In order to promote unidirectional heat flow during solidification, a copper chill was used, with the heat-extracting surface being polished. Experiments were performed with hypoeutectic Al–5 wt% Si and Al–9 wt% Si alloys (made from commercially pure materials).

ISSN 2176-5480

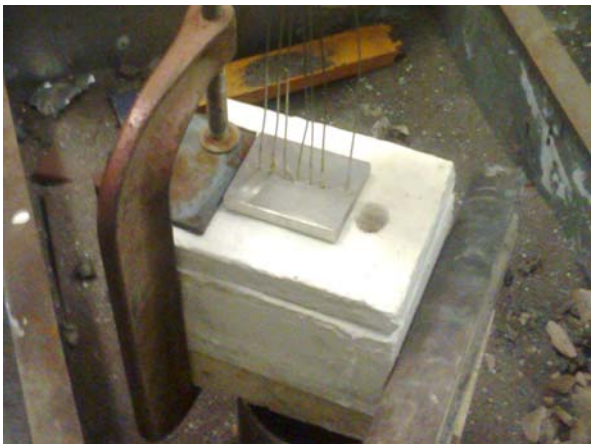

Figure 1. Horizontal solidification setup.

Each alloy was melted in an induction furnace until the melt reached a predetermined temperature. It was then stirred, degassed and poured into the casting chamber with a melt superheat of about 10% above the *liquidus* temperature. Temperatures in the casting were monitored during solidification via the output of a bank of type K thermocouples (sheathed in 1.5mm o.d. stainless steel protection tubes) accurately located with respect to the metal/mold interface.

Transversal specimens were cut from central pieces of the casts. Each specimen was then polished until microstructure was revealed. Half of the whole solidified casting was etched sideways using a solution of 5mL HF, 30 mL HNO_3, 60 mL HC*l* e 5 mL H_2O to reveal the macrostructure of grain growth (to verify a columnar structure in the cast).

An image processing system was then used to measure the average tertiary dendrite arm spacing (20 measurements for each selected position from the metal/mold interface).

For better controlling of the casting process, hardness profile along the preferential solidification direction was evaluated using Vickers (ASTM International, 2004) scale, according to the test conditions that follow in Tab. 1. At least 10 measurements for each specimen were performed, being the final result the average values and their standard deviations.

Table 1. Hardness tests conditions.

Hardness Scale	Test Conditions
Vickers $HV_{0.2}$	Test Force, F 200 gf

2.2 Machining tests

After being cast, Al-5.0wt.%Si ingots were sectioned into five segments with growing thickness from the copper mold along the solidification direction. Each segment was squared up and drilled in order to be suitable to the machining tests, as it can be seen in Fig. 2.

Machining tests were held on a Mori Seiki SV-40 vertical machining center CNC GE Fanuc MSC-518, using a 12 mm diameter square end mill (maker's code HM90 E90A-D12-1-C16) and ISO HM N10-N30 grade uncoated carbide inserts (maker's code HM90 APCR 100304PDFR-P IC28). Following the manufacturer instructions (ISCAR Metals, 2012), cutting speed, feed per tooth and axial depth of cut were kept, respectively equal to 490 m/min, 0.1 mm and 1.0 mm, while radial depth of cut was 12 mm (full immersion), as shown in Tab. 2. Blaser B-Cool 655 synthetic cutting fluid was employed.

ISSN 2176-5480

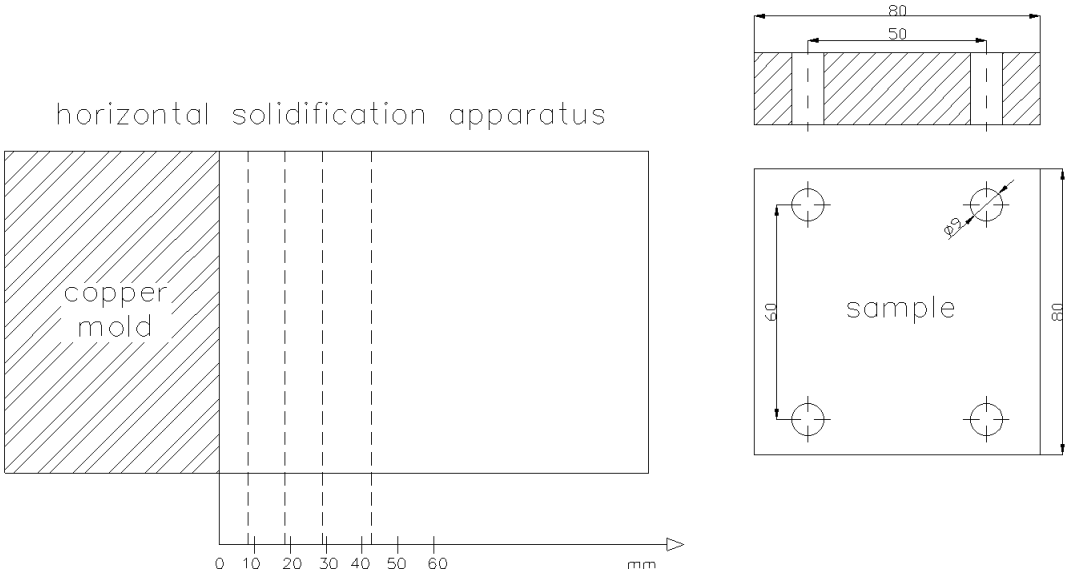

Figure 2. Machining tests sampling, considering directional solidification.

Table 2. Tooling and cutting parameters employed in the machining tests.

Tooling	Holder	HM90 E90A-D12-1-C16
	Insert	HM90 APCR 100304PDFR-P IC28
Parameters	Cutting Speed	490 m/min
	Feed per Tooth	0.1 mm
	Axial Depth of Cut	1.0 mm
	Radial Depth of Cut	12 mm

All measurements of cutting forces were made setting each sample on a Kistler 9257B multicomponent dynamometer connected to a Kistler 5019B charge amplifier and a NI PCI-6025E multifunctional data acquisition board. The NI LabVIEW 8.5 software was used to process signals received by the PC, as it follows in Fig. 3, where *Fx*, *Fy* and *Fz* are the main cutting force components measured over the workpiece. Acquisition rate was fixed as 600 Hz, and a 300 Hz low pass filter was applied.

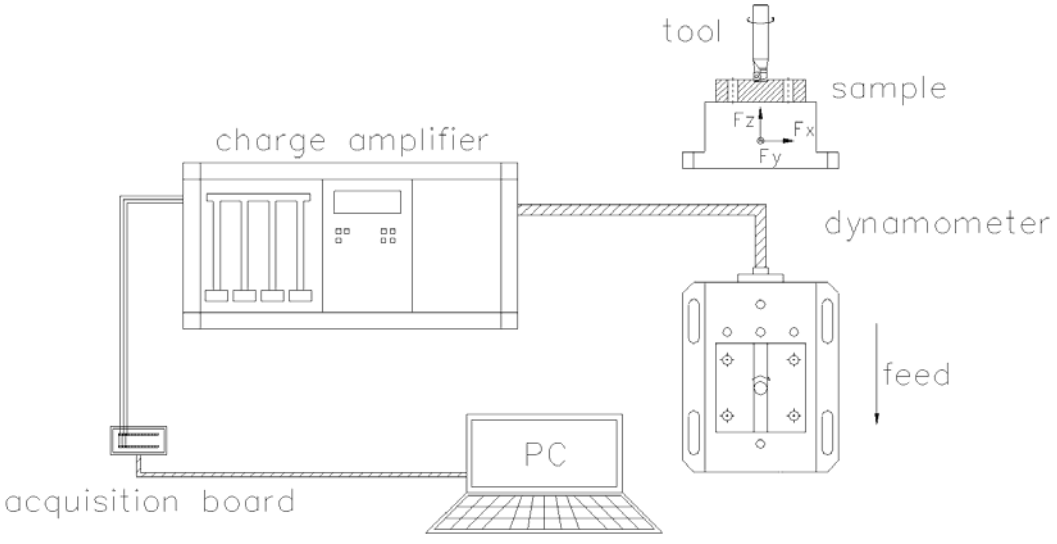

Figure 3. Setup for cutting force measurements.

ISSN 2176-5480

Instantaneous total cutting force *F* is a resultant of the vectorial sum of *Fx*, *Fy* and *Fz* main components, as follows in Eq. (1). Its root mean square (RMS) value can be calculated by Eq. (2), where *N* is the number of measurements.

$$F = \sqrt{F_x^2 + F_y^2 + F_z^2} \tag{1}$$

$$F_{RMS} = \sqrt{1/N \sum_{i=1}^{N} F^2} \tag{2}$$

3. RESULTS AND DISCUSSIONS

3.1. Aspects on Solidification of Al-5.0 and 9.0wt%Si alloys

Aspects involving kinetic variables along transient solidification of hypoeutectic Al-Si alloys (i.e., tip cooling rate, $\dot{T}$ and tip growth rate, V_L) are already known as established by Goulart and collaborators (2006 and 2007). However, in the present study such parameters had to be examined again in order to allow general experimental inter-relations to be established, which means determining solidification processing variables as a way to gain insight into the Al-Si foundry process, by preprogramming solidification in terms of some particular level of hardness or milling cutting force for both Al-Si alloys.

The thermal data from the cooling curves (Figs. 4a and 4b) were used in the determination of solidification thermal parameters, which are tip growth rate (V_L) and cooling rate ($\dot{T}$) along the Al-Si casting length (see Figs 5a and 5b). These parameters were found out by considering the thermal data recorded immediately after the passage of the *liquidus* isotherm by each thermocouple. The time (t) intervals corresponding to the passage of the *liquidus* isotherm by each thermocouple and the beginning of cooling launch (when the melt temperature was about 690°C and 650°C for Al-5.0 and 9.0wt%Si alloys, respectively, i.e., time (t) =0) have been determined. A plot of position of each thermocouple against these time intervals has been generated. Tip growth rates were then determined based on the time-derivative of the fitting function representing such experimental plot. Higher V_L and $\dot{T}$ values are associated with positions close to the surface of the Al-Si alloy casting in contact with the copper chill, decreasing along the casting length as can be seen in Figs 5a and 5b. It can be seen in Fig. 5b that the experimental set-up allowed, for instance, a considerable range of cooling rates to be attained along the Al-5.0wt%Si alloy casting length (in the range 2- 14 K/s).

The analysis of solidification thermal variables was limited to the region where columnar grains have developed, which means 40mm and 35mm from metal/chill interface for the Al-5.0 and 9.0wt%Si alloys, respectively (see Fig. 6).

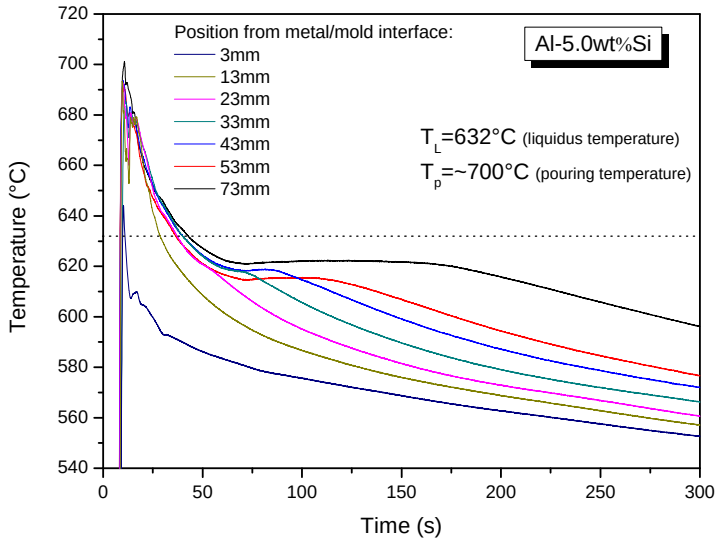

(a)

Figure 4. Cooling curves registered during unsteady-state horizontal solidification of the (a) Al-5.0wt. %Si and (b) Al-9.0wt. %Si alloys against copper mold.

ISSN 2176-5480

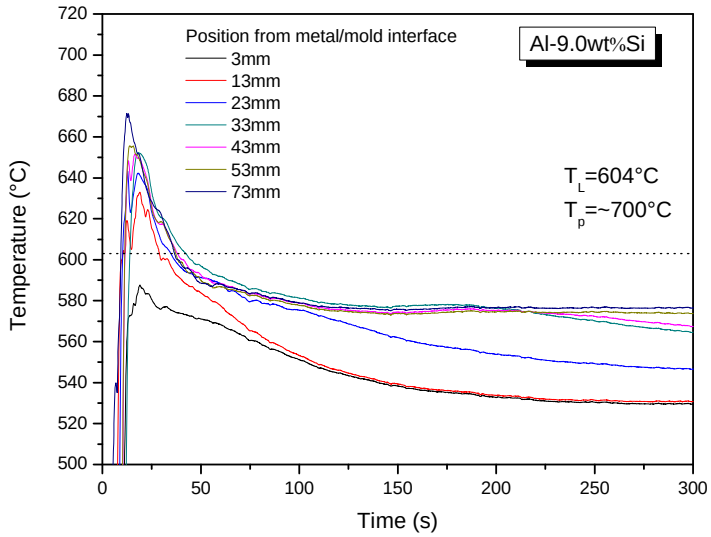

(b)

Figure 4. Continuing.

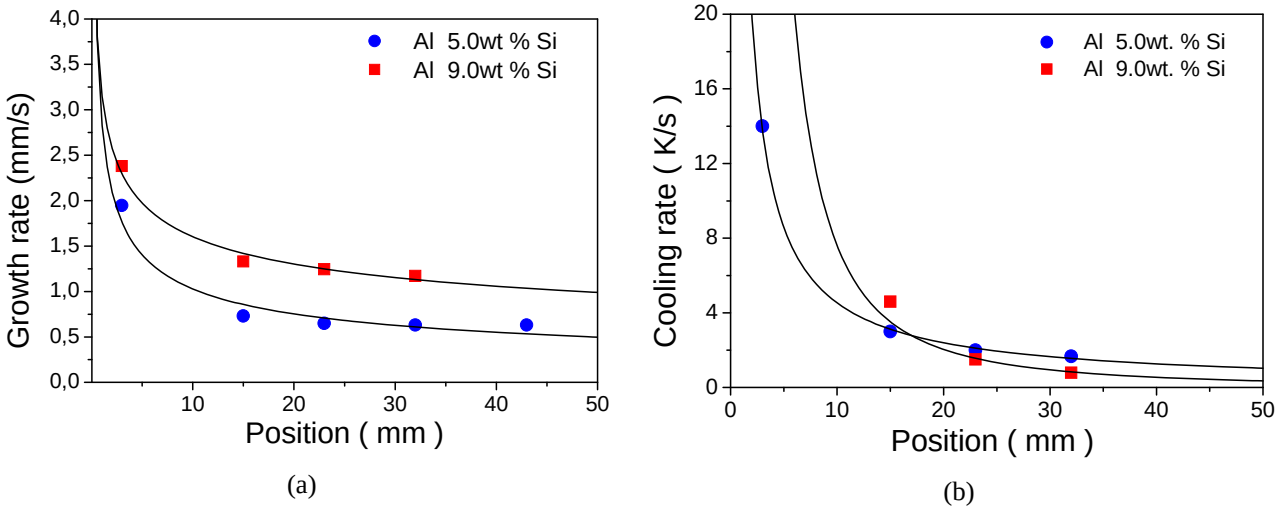

(a) (b)

Figure 5. (a) Tip growth rate and (b) cooling rate evolutions for both Al-5.0wt. %Si and Al-9.0wt. %Si alloys.

Fig. 6 depicts the macrostructure of the directionally solidified Al-Si alloys castings. It can be seen that a columnar macrostructure does not prevailed along the entire casting with a clear and narrow transition in both examined cases, anticipated in the case of higher Si content alloy.

ISSN 2176-5480

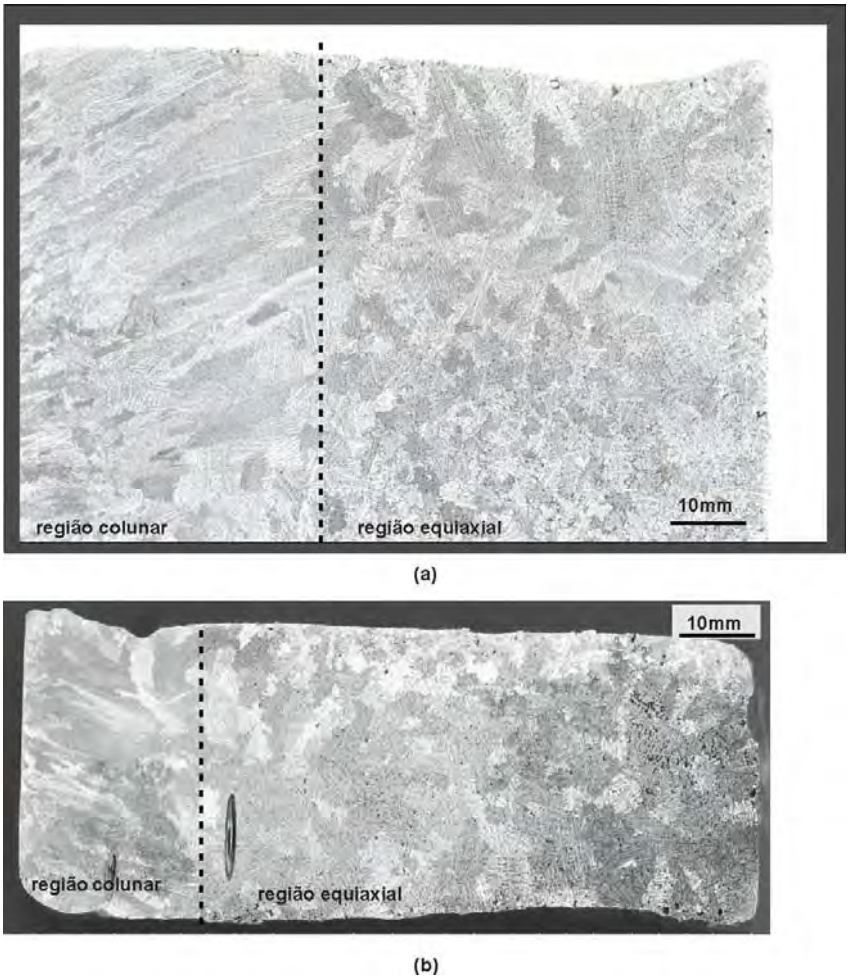

Figure 6. Structure of grains fond along horizontally solidified (a) Al-5.0wt.%Si and (b) Al-9.0wt.%Si alloys castings.

Typical cross-section microstructures of Al–5 wt.% Si and Al–9 wt.% Si alloys castings are shown in Fig 7. The main structure of hypoeutectic non-modified Al–Si alloys consists of a large quantity of needle-like silicon crystals set in an Al-rich dendritic matrix. It can be seen that, as expected, increasing the solute content (from 5wt% to 9wt%) larger eutectic areas are developed (corresponding to grey areas in Fig. 7).

(a) Al-5.0wt. %Si – cross section	(b) Al-9.0wt. %Si – cross section
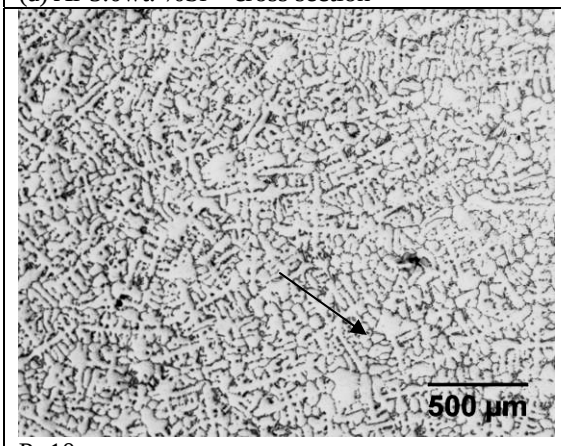	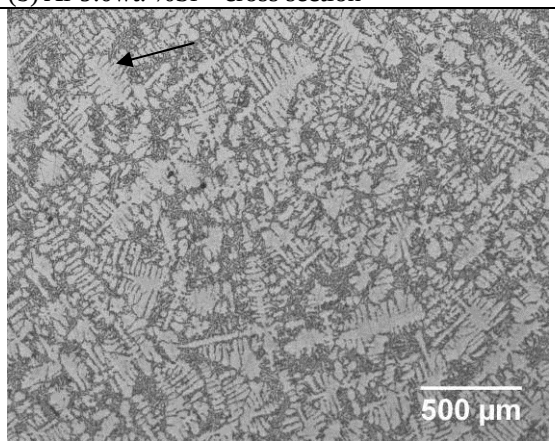
P=10mm	P=10mm

Figure 7. Typical microstructures corresponding to the position at 10mm from the casting cooled surface. Arrows indicate some of the tertiary branches.

ISSN 2176-5480

Average values of tertiary dendrite arm spacing and their standard deviations for each corresponding position can be seen in Fig. 8 for both evaluated Al-Si alloys. It is well known that tertiary branches grow past initiating secondary branches and may go on to become primary arms. Goulart et al. (2006) observed that increasing the silicon content finer secondary dendritic arm spacings may be obtained. The same trend may be applied in the case of tertiary dendritic growth under horizontal directional solidification.

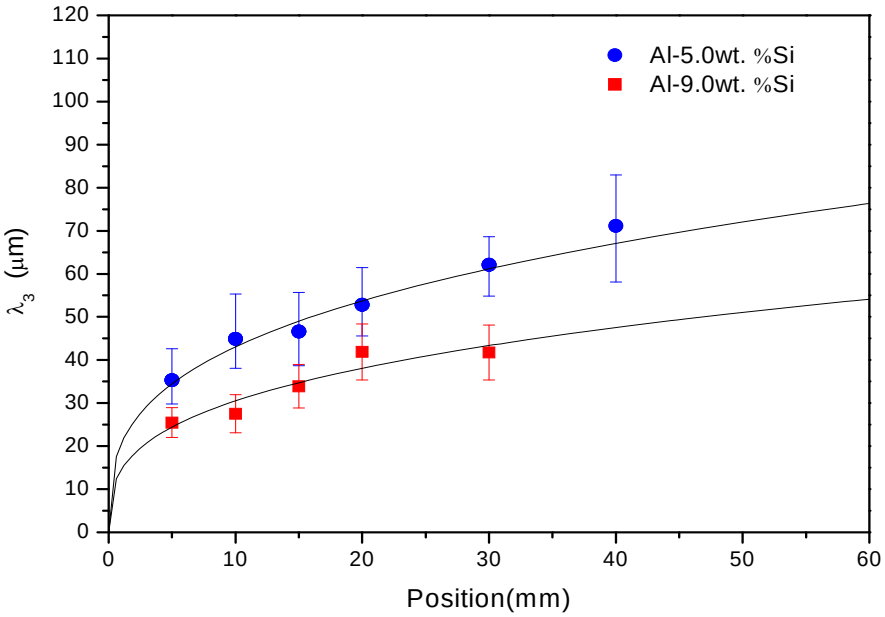

Figure 8. Development of tertiary dendrite arm spacing along positions of the Al-5.0wt%Si and Al-9.0wt%Si alloys castings.

3.2. Hardness and Cutting force obtained for directionally solidified Al-5.0 and 9.0wt%Si alloys

Fig. 9 shows the microhardness variation as a function of position (P) from metal/chill interface. The first regions of the Al-Si castings present finer microstructure, i.e., lower tertiary dendrite arm spacing values. This feature increases microhardness values corresponding to such positions (P<20mm, see Fig. 8). For higher positions and larger λ_3 values, microhardness decreases. As expected, higher microhardness values were determined for the alloy with higher silicon content.

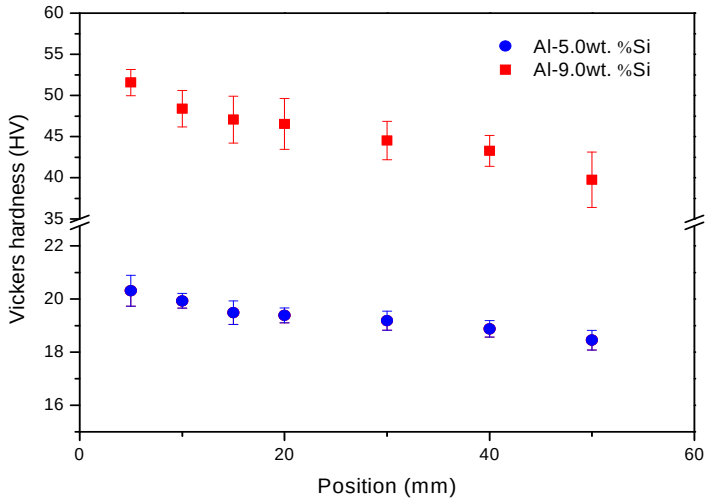

Figure 9. Vickers Hardness as a function of positions for the Al-5.0wt%Si and Al-9.0wt%Si alloys castings.

Figure 10 presents total cutting force F_{RMS} measured during end milling tests regarding the distance between the corresponding sample and the copper bloom mold surface belonging the horizontal directional solidification apparatus.

ISSN 2176-5480

The closer to copper block surface, the higher forces are required on corresponding sample machining, as more refined dendrite microstructure and so harder stock are found. Total cutting force (RMS) falls from more than 120 N reaching near 40 N around 30 mm far from the mold. Curiously, this value seems not to vary too much at larger distances. Santos and co-authors (2007) determined turning cutting forces of about 55 N corresponding to Al-12 and 16wt%Si alloys. Such value is in the same order of magnitude as those obtained in this work. Although much higher silicon content was tested in the mentioned study, size of Si particles is probably larger than that we have found once Al-12 and 16wt%Si alloys were solidified against gray cast iron chill mold, which present lower thermal diffusivity than copper.

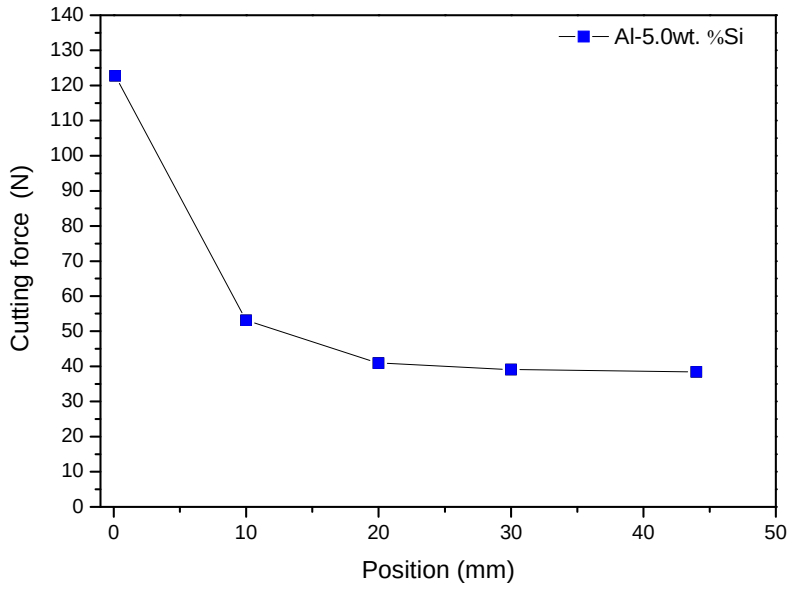

Figure 10. Total milling cutting force against relative position along the Al-5.0wt%Si alloy casting.

Figure 11 depicts the experimental inter-relations found for cutting force and scale of microstructure ($\lambda_3^{-1/2}$) and for microhardness and scale of microstructure. The established relations are Hall-Petch like ($HV=HV_0+k.\lambda_3^{-1/2}$) even though cutting force is not exactly a mechanical property. Thus, in this case a correlation will not be proposed, being inserted in Fig. 11 only a trend. It can be clearly observed that microhardness and cutting force evolve proportionally for the range of $\lambda_3^{-1/2}$ from 0.10 to 0.20.

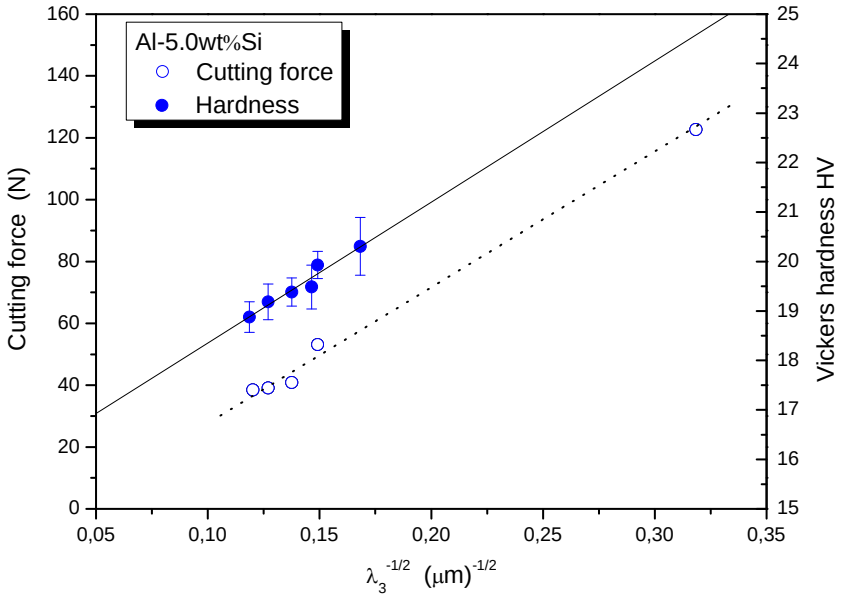

Figure 11. Experimental inter-relations of milling cutting force and hardness as a function of the microstructural parameter tertiary dendritic spacing, λ_3, derived for the as-cast Al-5.0wt. %Si alloy.

ISSN 2176-5480

4. CONCLUSIONS

From the experimental results acquired in this work, the following conclusions can be done:

- Dendritic arrangement is formed by dendritic spacing of high and low order, being considered in the present study those of higher order, which are tertiary dendritic spacing.
- Tip cooling rate varied from 2.0 and 12.0 K/s for the evaluated as-cast Al-Si alloys. This variation seems to provoke a variation in the size of microstructure, which is translated by a spectrum of λ_3 values from 70 μm to 25 μm.
- The microhardness values for the Al-9.0wt%Si alloy (from 40 to 52 HV) were found to be superior to those measured for the Al-5.0wt%Si alloy (from 18 to 20 HV).
- Finer Al-5.0wt%Si as-cast microstructure requires maximum cutting force (~ 120 N). However, higher values for tertiary dendritic spacing (~ 50 μm) clearly reduce this demand to of about 40 N.
- Parallel curves for hardness and cutting force both against $\lambda_3^{-1/2}$ seem to indicate that those characteristics are closely related.

5. ACKNOWLEDGEMENTS

The authors would like to thank all staff from Machining Materials Laboratory at University of Campinas (UNICAMP) for the support during the tests, Iscar Brasil for providing the cutting tools and Blaser Swisslube for cutting fluid supply. Thanks also the financial support provided by FAPESP (The Scientific Research Foundation of the State of São Paulo, Brazil) and to PIBIC/CNPq/UFSCar for granting a scholarship.

6. REFERENCES

ASTM International, 2004. *E92-82*: Standard Test Method for Vickers Hardness of Metallic Materials. West Conshohocken, 32 p.

Campbell J, 2003. *Castings*. 2nd ed. Oxford, Great Britain: Butterworth-Heinemann.

Chemingui, M; Khitouni, M; Jozwiak, K; Mesmacque, G and Kolsi,A., 2010., "Characterization of the mechanical properties changes in an Al–Zn–Mg alloy after a two-step ageing treatment at 70 and 135 °C", *Materials and Design*, Vol. 31, p. 3114.

Donelan, P., 2000, "Modelling microstructural and mechanical properties of ferritic ductile cast iron". *Materials Science and Technology*, Vol. 16, p. 261.

Goulart, P. R.; Osório, W. R.; Spinelli, J. E.; Garcia, A., 2007. "Dendritic Microstructure Affecting Mechanical Properties and Corrosion Resistance of an Al-9 wt% Si Alloy". *Materials and Manufacturing Processes*, Vol. 22, p. 328.

Goulart, P; Spinelli, J E; Osório, W R; Garcia, A., 2006. "Mechanical properties as a function of microstructure and solidification thermal variables of Al Si castings". *Materials Science & Engineering. A*, Vol. 421, p. 245.

ISCAR Metals, 2012. Milling Tools. 27 Aug. 2012 <http://www.iscar.com/Catalogs/>.

Osório, W R; Garcia, L R.; Goulart, P R.; Garcia, A., 2007. "Effects of eutectic modification and T4 heat treatment on mechanical properties and corrosion resistance of an Al 9wt%Si casting alloy". *Materials Chemistry and Physics*, Vol. 106, p. 343.

Osório, WR; Goulart, PR; Santos, GA; Moura Neto, C and Garcia, A., 2006. "Effect of Dendritic Arm Spacing on Mechanical Properties and Corrosion Resistance of Al9wtpctSi and Zn27wtpctAl Alloys", *Metallurgical and. Materials Transactions A*, Vol. 37, p. 2525.

Rathod, NR and Manghani, JV., 2012. "Effect of modifier and grain refiner on cast Al-7Si aluminum alloy: a review ", *International Journal of Emerging Trends in Engineering and Development*, Vol. 5, p. 574.

Santos, GR; Costa, DD; Amorim, FL; Torres, RD., 2007. "Characterization of DLC thin film and evaluation of machining forces using coated inserts in turning of Al–Si alloys", *Surface & Coatings Technology*, Vol. 202, p. 1029.

Santos, GA; Neto, C.M.; Osório, WR and Garcia, A., 2007. "Design of Mechanical Properties of a Zn27Al Alloy Based on Microstructure Dendritic Array Spacing", *Materials and Design*, Vol. 28, p. 2425.

Sokołowski, JH ; Szablewski, D ; Kasprzak, W. ; Ng, EG ; Dumitrescu, M., 2006. "Effect of tool cutter immersion on Al-Si bi-metallic materials in High-Speed-Milling", *Journal of Achievements in Materials and Manufacturing Engineering*, Vol. 17, p. 15.

Trent, E.M. and Wright, P.K., 2000. *Metal Cutting*. Butterworth-Heinemann, Woburn, 4th edition.

ISSN 2176-5480

Wang, Y; Liu, B; Song, J; Yan, X and Wu, K., 2012. "Study on the wear mechanism of PCD tools in high-speed-milling of Al-Si alloys", *Advanced Materials Research*, Vol. 381, p. 16.

Ye, H., 2003. "An Overview of the Development of Al-Si-Alloy Based Material for Engine Applications", *Journal of Materials Engineering and Performance*, Vol. 12, p. 288.

Zedan, Y; Samuel, FH; Samuel, AM; Doty, HW., 2010. "Effects of Fe intermetallics on the machinability of heat-treated Al–(7–11)%Si alloys", *Journal of Materials Processing Technology*, Vol. 210, p. 245.

Zimmerman, C., Boppana, S.P. and Katbi, K., 1990. "Machinability Test Methods". In: *ASM Metals Handbook - v. 16*.

7. RESPONSIBILITY NOTICE

The authors Eduardo Tadeu Schiavon Gandini, Bruno Monte Carmelo Donadoni, Armando Ítalo Sette Antonialli and José Eduardo Spinelli are the only responsible for the printed material included in this paper.